Jpn. J. Appl. Phys. Vol. 41 (2002) pp. 5986–5990
Part 1, No. 10, October 2002
©2002 The Japan Society of Applied Physics

Synthesis of Bi–Lu-Substituted Iron Garnet Films for Visualization of Magnetic Flux in High-T_c Superconductors

Nobuyasu ADACHI*, Keiji OBATA, Takashi OKUDA, Takato MACHI[1] and Naoki KOSHIZUKA[1]

Department of Material Science and Engineering, Nagoya Institute of Technology, Gokiso-cho, Showa-ku, Nagoya 466-8555, Japan
[1]*Superconductivity Research Laboratory, International Superconductivity Technology Center, 1-10-13 Shinonome, Koto-ku, Tokyo 135-0062, Japan*

(Received April 10, 2002; accepted for publication July 2, 2002)

In order to visualize the magnetic flux that penetrates into high-T_c superconductors with high spatial resolution, epitaxial growth of the in-plane magnetic Bi–Lu-substituted iron garnet films was investigated. The ratio of increments of Faraday rotation to magnetic field increased to -13 deg/(cm·Oe) by Bi and Ga substitutions. The as-grown films showed a perpendicular magnetic anisotropy. The appropriate conditions for annealing treatments that change the perpendicular magnetic anisotropy into an in-plane magnetic anisotropy were investigated. Then, the annealed $(BiLu)_3(FeGa)_5O_{12}$ film clearly showed a high resolution image of the magnetic flux that penetrates into the $NdBa_2Cu_3O_{7-\delta}$ high-T_c superconductor at temperatures between 5 K and 100 K, and the behavior of the magnetic flux penetrating the microcracks less than 5 μm in width was successfully captured; the magnetic flux depends on external magnetic field and temperature.
[DOI: 10.1143/JJAP.41.5986]

KEYWORDS: magnetooptical imaging, magnetic flux, magnetic garnet, LPE, in-plane magnetic anisotropy, high-T_c superconductor

1. Introduction

For practical applications of high-T_c superconductors, it is important to characterize the behavior of magnetic flux that penetrates superconducting materials in applied magnetic fields. One of the most attractive characterization techniques is visualization of magnetic flux using magnetooptical (MO) effects. High-contrast observations of magnetic flux density using a magnetic garnet film have been reported in the last ten years.[1–3] The use of magnetic garnet films has advantages over the magnetic flux observation in high-T_c superconductors because of their (1) high Curie temperature T_c above 550 K and (2) large Faraday effects which give high contrast to different magnetic flux densities. These properties of magnetic garnet films enable observation of a wide dynamic range of the magnetic fluxes that penetrate into high-T_c superconductors in comparison with the observation using EuSe ($T_c = 5$ K) or EuO ($T_c = 69$ K).

Thin films with in-plane magnetic anisotropy enable high-resolution imaging of magnetic flux predicted to be less than 1 μm. However, it is difficult to synthesize a complete in-plane magnetic garnet film because the growth-induced magnetic anisotropy and crystalline magnetic anisotropy easily generate perpendicular magnetic domains. Yokoyama *et al.* reported for the first time the behavior a magnetic flux that penetrated into $YBa_3Cu_3O_x$ high-T_c superconductor using Bi-substituted YIG, a perpendicular magnetic film.[1] In this case, the magnetic domain wall limits the spatial resolution to 10–30 μm. There are several reported observations on the behavior of dynamical magnetic flux in high-T_c superconductors using in-plane magnetic garnet films in the last 10 years.[4–8] Recently, Johansen *et al.* have reported the observation of flux patterns in MgB_2 films by the MO imaging technique.[8] In these reports, the films used for magnetic flux observation were prepared by the liquid phase epitaxy (LPE) technique. For the optical devices, the LPE technique has great advantages over conventional techniques in achieving two dimensional crystal growth and an optically smooth surface of the film. In addition, various growth parameters such as melt composition, growth temperature and rotation speed enable controls of the magnetic and magnetooptical properties of films.[9] In order to fabricate in-plane magnetic films, we recently reported the in-plane magnetic anisotropy of the Nd- and Pr-substituted iron garnet films prepared by the LPE technique.[7] Nd- and Pr-substituted films exhibited a negative growth-induced magnetic anisotropy which leads to an in-plane magnetic anisotropy.[10] We utilized the growth-induced magnetic anisotropy for the in-plane magnetic film and tried to prepare a film with large amounts of Pr and Nd ions. In such a film, the energy of the growth-induced magnetic anisotropy is sufficiently large at room temperature in comparison with other magnetic anisotropies such as the crystalline magnetic anisotropy and stress-induced magnetic anisotropy. However, with decreasing temperature, the crystalline magnetic anisotropy energy due to increment of rare-earth ions.[11] This increased anisotropy energy may compete with growth-induced magnetic anisotropy, which causes non-linear magnetization curve. We have observed steplike magnetization curve for the $(NdBiLu)_3Fe_5O_{12}$ film which was grown by LPE technique (see Fig. 1). At room temperature, the magnetization of the film linearly changes up to saturation in proportion to the magnetic field; however, the film shows a steplike magnetization curve at 77 K. At the present stage, the origin of the anomaly of the magnetization curve has not yet been clarified in detail. One of the possible reasons is that the increment of the magnetic moment of rare-earth ions affects the magnetic anisotropy with decreasing temperature. In order to avoid the influence of the crystalline magnetic anisotropy due to rare-earth ions, we chose the synthesis of the Nd- and Pr-ion-free magnetic garnet film, $(BiLu)_3(FeGa)_5O_{12}$ (BLIG). $Lu^{3+}(4f^{14})$ is magnetically inactive. Bi substitution increases the degree of Faraday rotation. The dilution of Fe ions with Ga ions results in a reduction of the magnetic field to saturate magnetization, which increases the rate of increase in the degree of Faraday rotation against the magnetic field. As-grown BLIG films show perpendicular magnetic anisotropy due to positive

*E-mail address: nadachi@mse.nitech.ac.jp

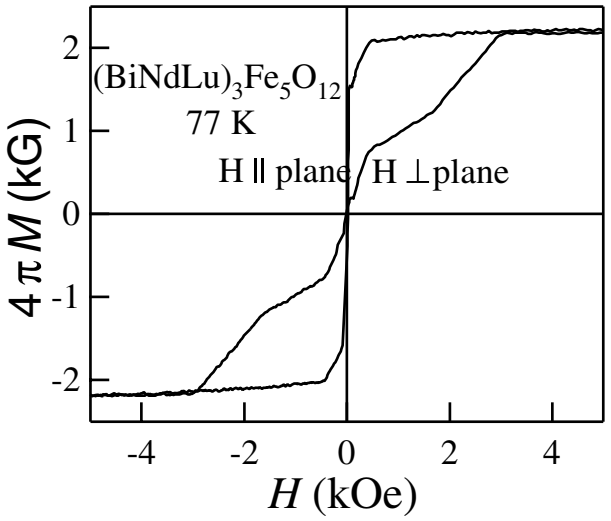


Fig. 1. Magnetic hysteresis curve for $(BiNdLu)_3Fe_5O_{12}$ film prepared by the LPE technique. Measurements were performed at 80 K. The magnetization curve is steplike.

growth-induced magnetic anisotropy. We expect that shape magnetic anisotropy causes the in-plane magnetic anisotropy of the film after removing the growth-induced anisotropy. In this paper, we report the detailed procedure for synthesizing the in-plane magnetic film of BLIG.

2. Experimental

The films were grown on $Gd_3Ga_5O_{12}$ (111) substrates ($a_s = 12.383$ Å). The melt compositions are summarized in Table I. Bi_2O_3 was used as the flux for BLIG. The preparation conditions are summarized in Table II. The substrate was horizontally dipped into the melt and was rotated at 100 rpm. The flux remains on the substrate when the substrate is extracted from the melts. In order to remove the flux residue on the film surface, the substrate was rotated at 500 rpm above the melt for 30 s. The films were annealed in air at temperatures between 850 and 1300°C. The temperature was increased up to the annealing temperature at a rate of 5°C/min in air and was kept for 2 h, then it was decreased at a rate of 5°C/min. The lattice mismatch (Δa_s) was determined by X-ray diffraction analysis. The compositions of the films were analyzed using an energy dispersive X-ray spectrometer (EDX). Faraday rotation was measured at a wavelength of 670 nm. The magnetization was measured with a vibrating sample magnetometer (VSM). The FMR was measured in the X-band microwave region. A polarized microscope was used for the observation of the magnetic flux that penetrated the high-T_c superconductor. We used a $NdBa_2Cu_3O_{7-\delta}$ (Nd123) specimen in this experiment. The specimen having $T_c \sim 94$ K, $J_c \sim 20$ kA/cm^2 (at 77 K in 0 Oe) was prepared by the self-flux method.[12] The $1.2 \times 1.0 \times 0.3$ mm^3 specimen, where c-plane was faced below the garnet, was mounted on the cold finger of a helium gas flow type optical cryostat and the temperature was varied from 5 K to 300 K. The film is grown on both sides of the substrate. For the observation of magnetic flux, one side of the film is polished and removed, then the other side is coated with gold for reflecting light. The gold-coated sides contacted with the specimen. The magnetic field was applied up to 8 kOe.

Table I. Composition of the melt (mol%) for BLIG film.

Melt	BLIG
Bi_2O_3	83.00
Fe_2O_3	13.99
Lu_2O_3	1.84
Ga_2O_3	1.17

Table II. Chemical analysis data and growth and annealing conditions for Bi–Lu-substituted iron garnet films.

	As-grown	Annealed
Lattice constant a (Å)	12.371	
Lattice mismatch Δa (Å)	0.002	
Thickness (μm)	10.4	
[Bi] (f./u.)	0.68	0.65
[Ga] (f./u.)	0.96	0.97
Saturation temp. (°C)	969	—
Growth temp. (°C)	824	—
Annealing temp. (°C)	—	930

3. Results and Analysis

The saturated Faraday rotation angle θ_F of the BLIG film was -13×10^3 deg/cm, which did not change before and after annealing treatments. The increment ratio of the θ_F of the annealed films against the magnetic field was -13 deg/(cm·Oe).

As-grown BLIG films showed a perpendicular magnetic anisotropy and a labyrinth domain structure, as observed under a polarized microscope [see Fig. 2(a)]. Annealing treatments changed the magnetic anisotropy of the film. The labyrinth structure disappeared with annealing above 900°C for 1 h [see Fig. 2(b)]. Annealing above 1000°C induced grain nucleation, which resulted in a rough surface. Thus, the optimal annealing temperature was determined to be 930°C. Figure 3 shows the magnetic hysteresis loops of the as-grown and annealed BLIG films. The magnetization of the annealed film easily saturates below 200 Oe in the magnetic field parallel to the film, which indicates that the magnetic anisotropy of the film changed into an in-plane magnetic anisotropy after the annealing treatment. From the saturation

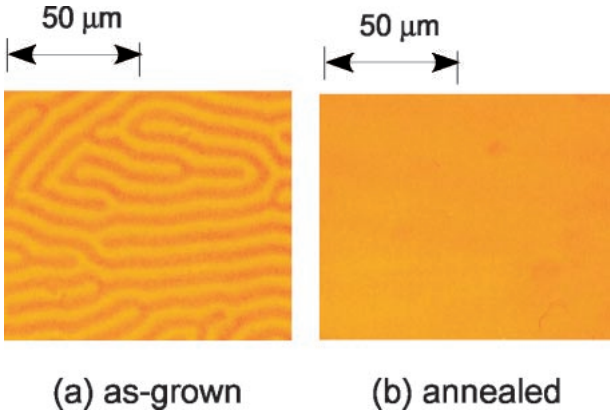


Fig. 2. Micrograph of the domain structure of the BLIG film. The labyrinth pattern is clearly observed in (a) as-grown film and the domain pattern disappears in (b) the film annealed at 930°C.

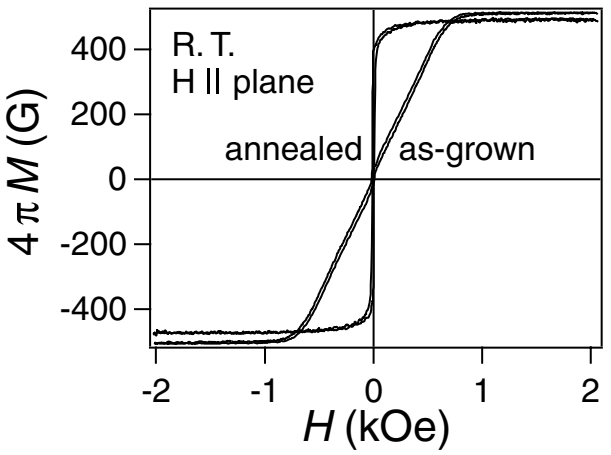


Fig. 3. Magnetic hysteresis loops of as-grown and annealed BLIG films with an applied magnetic field parallel to the plane at room temperature. It is clear that the annealed film shows in-plane magnetic anisotropy.

magnetization and ferromagnetic resonance fields, the uniaxial magnetic anisotropy energy K_u of the as-grown film at room temperature was estimated to be $+6.1\times 10^3$ erg/cm^3 using

$$K_u = \frac{H_A M_S}{2} + \frac{5}{18} K_1,$$

$$H_A = \frac{2}{3}(H_\parallel - H_\perp) + 4\pi M_S,$$

where K_1 is the cubic crystalline anisotropy. The value of K_1 ($= -2.0 \times 10^3$ erg/cm^3) for $Y_{3-x}Bi_xFe_{5-y}Ga_yO_{12}$ ($x = 0.7$, $y = 1$) is used[13,14] on the assumption that there is no remarkable difference in effect between Y and Lu. H_A is the anisotropy field, $H_\parallel$ and $H_\perp$ are the parallel and perpendicular resonance fields. The stress-induced anisotropy $K_u(\lambda)$ is estimated to be -7.14×10^2 erg/cm^3 using

$$K_u(\lambda) = -\frac{3}{2}\frac{E}{1-\mu_{111}}\frac{\Delta a}{a}\lambda_{111},$$

where E and μ_{111}, are the Young modulus ($= 2.05\times 10^{11}$ erg/cm^3) and Poisson constant ($= 0.30$) of pure $Y_3Fe_5O_{12}$, respectively.[14] λ_{111} is the magnetostriction constant of the [111]-oriented film (-1.34×10^{-6}).[13,14]

K_u of the annealed film at room temperature was determined to be -11.4×10^3 erg/cm^3. The negative sign confirms the in-plane magnetic anisotropy of the film. The magnetic properties of the as-grown and annealed films are summarized in Table III.

The change of the magnetic anisotropy can be considered as follows; the magnetic anisotropies of the film consist of the growth-induced magnetic anisotropy, stress-induced anisotropy, crystalline magnetic anisotropy and shape magnetic anisotropy. The energies of these anisotropies except for the growth-induced anisotropy are effective for the in-plane magnetic anisotropy of the film. For the case of the as-grown film, the dominant magnetic anisotropy is considered to be the growth-induced magnetic anisotropy. After the growth-induced anisotropy was removed by annealing treatments, other magnetic anisotropy energies caused the change from the perpendicular magnetic anisotropy to the in-plane magnetic anisotropy.

Table III. Magnetic properties of BLIG as-grown and annealed films.

	As-grown		Annealed	
	R.T.	77 K	R.T.	77 K
$4\pi M_s$ (G)	498	705	475	650
$H_\parallel$ plane (Oe)	3446	3304	3002	3246
$H_\perp$ plane (Oe)	3560	3646	4577	3847
K_u (10^3 erg/cm^3)	7.3	12.9	−11.4	5.9

"$H_\parallel$ plane (Oe)" and "$H_\perp$ plane (Oe)" denote the FMR resonance fields in the the parallel and perpendicular magnetic fields, respectively.

With decreasing temperature, K_u increases. At a temperature of 78 K, K_u of the as-grown BLIG was $+12.9 \times 10^3$ erg/cm^3 and that of the annealed film was $+5.9 \times 10^3$ erg/cm^3. According to the study by Hansen *et al.*, the uniaxial anisotropy of Lu–Bi films increases with decreasing temperature due to the increments of growth-induced anisotropy.[15] In our case, the growth-induced anisotropy may not be completely removed with annealing, which probably results in the increment of K_u. The sign of K_u changed to positive at 78 K, however, the anisotropy field of $2K_u/M_s$ is smaller than the demagnetizing field of M_s/μ_0 (μ_0 is permeability of vacuum), which indicates that the film maintains the in-plane magnetic anisotropy. In comparison with the increase of the saturation magnetization at low temperature, the shift of the ferromagnetic resonance field is small, which may lead to increasing K_u.

The hysteresis loop of the Faraday rotation at 635 nm is shown in Fig. 4. The saturation magnetic field was about 1000 Oe and the ratio of increments of Faraday rotation against the magnetic field was 13 deg/(cm·Oe) for the annealed film.

By using the annealed BLIG film, the images of magnetic flux that penetrated into Nd123 single crystal were successfully visualized with high spatial resolution [see Figs. 5(a)–5(f)]. The rectangular Nd123 single crystal was cooled to 5 K in a zero magnetic field. Then, a magnetic field was applied perpendicularly to the (010) plane of the specimen up to 8 kOe. With increasing magnetic field, the

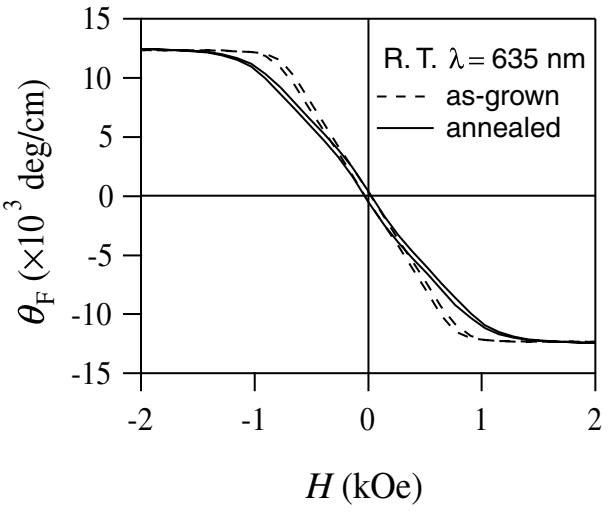


Fig. 4. Faraday hysteresis loops of as-grown and annealed BLIG films at a wavelength of 635 nm. The saturation magnetic field of the annealed film is about 1000 Oe and the ratio of the increments of the Faraday rotation against the magnetic field is 13 deg/(cm·Oe).

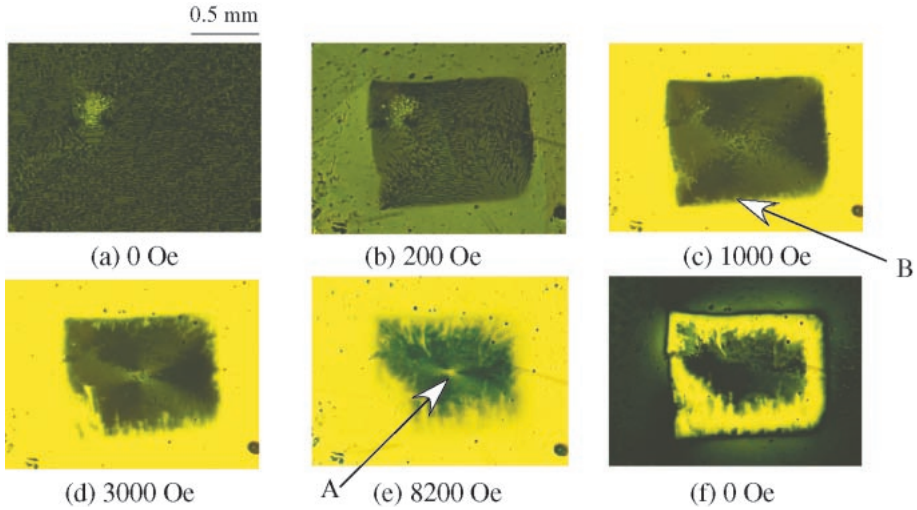


Fig. 5. Images of the magnetic flux that penetrated into the single-crystal superconductor Nd123 observed at 5 K using the annealed BLIG film. The garnet film was placed onto the ac-plane of the specimen and the magnetic field was applied after zero-field cooling [see (a), (b) and (c)], then the magnetic field returned to zero (d).

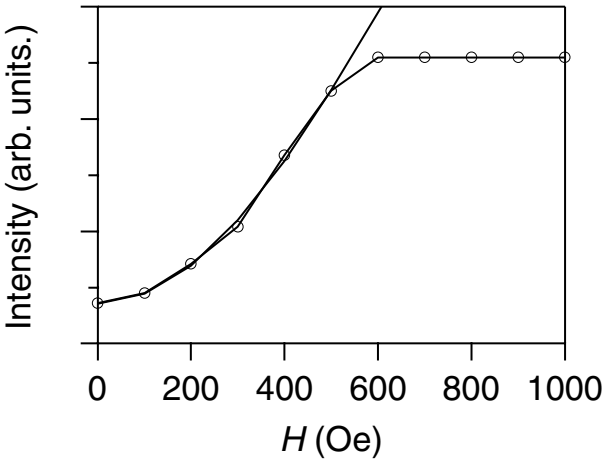


Fig. 6. Light intensity transmitted in the garnet film vs applied magnetic field. Solid circles are experimental results and solid line represents the fitting curve expressed by $I = I_0 - A\cos^2\theta_F(H)$. Light intensity seems to saturate above 500 Oe due to the charge saturation of CCD detector.

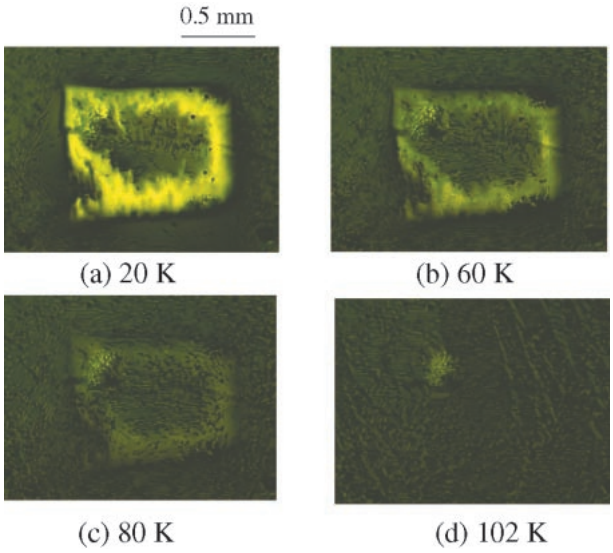


Fig. 7. Temperature dependence of the remanent magnetic flux in the Nd123 specimen. With increasing temperature, the penetrated magnetic flux around the edge of the specimen decreases and it disappears above 100 K.

area of the bright part of the specimen increased. The bright part of the specimen corresponds to the area where magnetic flux penetrated the specimen. The dark part is the area where magnetic flux is excluded due to the Meissner effect. When the applied magnetic field was decreased to zero from 8 kOe, the magnetic flux remained at the edge and around the cracks of the specimen [see Fig. 5(d)]. The spatial resolution is estimated to be about 1 μm in these images, which is difficult to achieve by using perpendicular magnetic films. The field dependence of the intensity I of the transmission light through the garnet film is shown in Fig. 6. The intensity at zero magnetic field is considered to be the background intensity at exposure time of 3 s. The solid line indicates experimental results and the dashed line indicates the fitting curve using $I = I_0 - A\cos^2\theta_F(H)$, where I_0 and A are the initial light intensity and fitting coefficient, respectively. The light intensity of the experimental result seems to be saturated above $H = 600$ Oe, which is due to the charge saturation of the CCD detector. Taking this relation into account, magnetic flux density B that penetrated the specimen was estimated as follows: on the specimen, the applied magnetic field H_{ext} is modified by the shielding field H_{shield}, and the film picks up the modified $H_{mod} = H_{ext} + H_{shield}$ correspond to the penetrated magnetic flux density B ($= H_{mod}$). Thus, the magnetic flux density that penetrated around the center of the specimen in $H = 3000$ Oe [see Fig. 5(d)] can be estimated to be approximately $B = 400$ G. The magnetic flux that penetrated around the cracks outside the specimen is expected to be greater than $B = 600$ G because of the saturation of the CCD detector.

The temperature dependence of the trapped magnetic flux in zero magnetic field is shown in Fig. 7. The brightness of the edge of the specimen decreases with increasing temperature and the trapped magnetic flux was completely excluded at approximately 100 K.

4. Conclusions

The $(BiLu)_3(FeGa)_5O_{12}$ films were synthesized by the LPE technique. Annealing of the as-grown perpendicular magnetic film above 900°C remarkably reduced the size of the perpendicular magnetic domain and the perpendicular magnetic anisotropy of the film changed to the in-plane magnetic anisotropy (K_u changed from $+6.1 \times 10^3$ erg/cm^3 to -11.4×10^3 erg/cm^3 at room temperature.) By using this film, the visualization of the magnetic flux with a spatial resolution of approximately 1 μm revealed the behavior of the penetrated magnetic flux in the high-T_c superconductor in the temperature range between 5 K and 100 K.

Acknowledgements

The authors are grateful to Mr. Sakai and other staff of the Institute of Molecular Science for SQUID measurement.

1) Y. Yokoyama, Y. Suzuki, Y. Hasumi, H. Obara, T. Yosimi, Y. Kita, S. Kosaka and S. Yoshida: Jpn. J. Appl. Phys. **30** (1991) L1864.
2) S. Gotoh, N. Koshizuka, M. Yoshida, M. Murakami, H. Fujimoto and S. Tanaka: Supercond: Sci. Technol. **4** (1991) S226.
3) A. A. Polyanskii, X. Y. Cai, D. M. Feldmann and D. C. Lasrbalestier: *Proc. NATO Advanced Research Workshop on Ferrimagnetic Nano-Crystalline and Thin Film Magnetooptical and Microwave Materials* (Kluwer Academic, Dordrecht, 1999) NATO Science Series Vol. 72, p. 353.
4) L. A. Dorosinskii, M. V. Indenbom, V. I. Nikitenko, Yu. A. Ossip'yan, A. A. Polyanskii and V. K. Vlasko-Vlasov: Physica C **203** (1992) L149.
5) M. R. Koblischka, A. D. M. Muralidhar, N. Sakai and M. Murakami: Jpn. J. Appl. Phys. **37** (1998) L1227.
6) M. R. Koblischka, L. Pust, T. H. Johansen, B. Nilsson and T. Clawson: Physica C **331** (2000) 113.
7) N. Adachi, N. Nishioka, T. Hibi, T. Okuda, T. Takagi, T. Machi and N. Koshizuka: *Advances in Superconductivity XI* (Springer-Verlag, Tokyo, 1999) p. 275.
8) T. H. Johansen, M. Baziljevich, D. V. Shantsev, P. E. Goa, Y. M. Galperin, W. N. Kang, H. J. Kim, E. M. Choi, M.-S. Kim, S. I. Lee: Supercond. Sci. Technol. **14** (2001) 726.
9) T. Hibiya: Jpn. J. Cryst. Growth **22** (1995) 370 [in Japanese].
10) P. Hansen, C.-P. Klages and K. Witter: J. Appl. Phys. **60** (1986) 721.
11) S. E. Slusky, J. F. Dillon, Jr., C. D. Brandle, M. P. Norelli and V. J. Fratello: Phys. Rev. B **34** (1986) 7918.
12) S. Shibata, A. K. Pradhan and N. Koshizuka: Jpn. J. Appl. Phys. **38** (1999) L1169.
13) P. Hansen, K. Witter and W. Tolksdorf: Phys. Rev. B **27** (1983) 6608.
14) P. Hansen, K. Witter and W. Tolksdorf: J. Appl. Phys. **55** (1984) 1052.
15) P. Hansen, C.-P. Klages and K. Witter: J. Appl. Phys. **60** (1985) 5858.